

# Bacterial Adsorption to Smooth Surfaces: Rate, Extent, and Spatial Pattern

C. H. Nelson<sup>1</sup>  
*SRI International, Menlo Park, California 94025*

J. A. Robinson  
*Upjohn Company, Kalamazoo, Michigan 49001*

W. G. Characklis\*  
*Institute for Biological and Chemical Process Analysis,  
Montana State University, Bozeman, Montana 59717*

*Accepted for publication April 8, 1985*

The influence of bulk-water bacterial cell concentration and specific growth rate history on bacterial adsorption rates to surfaces was investigated using response surface analysis. A pure culture of *Pseudomonas* sp. 224S was grown in a chemostat and pumped into a continuous flow reactor where the bacteria were exposed to clean, glass surfaces under turbulent flow conditions for a period of six hours. Adsorption rate decreased approximately linearly with increasing specific growth rate history. Glass surfaces became saturated with 224S at ca. 0.1% coverage and the resulting spatial pattern of the adsorbed cells deviated from random in the direction of uniformity.

## INTRODUCTION

Bacterial adsorption to surfaces is of significant technical interest with respect to biodeterioration and biocatalysis. Biodeterioration refers to the reduced quality, performance, and/or lifetime of commercial products and process equipment as a result of the accumulation of biofilm.<sup>1</sup> Biocatalysis, on the other hand, takes advantage of similar biofilms to effect or hasten the rate of a reaction of significant commercial importance. Many variables can influence the accumulation of cells on surfaces. In this study, the concentration of cells in the bulk phase and the previous growth rate history of these cells were specifically investigated.

Bacterial accumulation on a surface is the net result of several processes: transport of bacteria to the surface, adsorption of bacteria to the surface, desorption of bacteria from the surface, and growth of the attached bacteria. The quantity measured in this study was the

net result of the adsorption and desorption processes and is referred to simply as adsorption rate. The effect of bacterial growth on surface accumulation rate measurements was negligible in this study for the following reasons: 1) substrate flux from the chemostat to the adsorption surface was negligible, 2) experiments were limited to six hours, and 3) potential colony forming units, PCFU (defined in the Procedures Section), were counted instead of cells.

Much of the published research on bacterial adsorption on surfaces has focused on mechanisms. The experiments reported herein focused on the rate and extent of bacterial adsorption in a manner similar to other recent studies.<sup>2,3</sup>

## EXPERIMENTAL SYSTEM

Figure 1 is a schematic of the experimental system. The continuous flow bacterial adsorption reactor (BAR) is enlarged to show detail. The chemostat and the BAR were Berzelius beakers each with a working volume of 450 mL. The BAR is a continuous flow system with bacteria and dilution water as the influent and effluent. Four glass microscope slides were suspended in the BAR by a frame consisting of silicon tubing and plastic supports. The relative turbulence of the BAR bulk water was kept constant in all experiments by maintaining the same stirrer setting. Dye tests indicated this stirring rate was adequate to assume complete and turbulent mixing of fluids. A specific value for the hydrodynamic shear stress at the glass surfaces could not be calculated due to the type of mixing employed in the BAR. Bacterial counts were made in the same relative location on each slide to minimize the effect of non-uniform turbulence over the slides. A pure

\* To whom correspondence should be addressed.

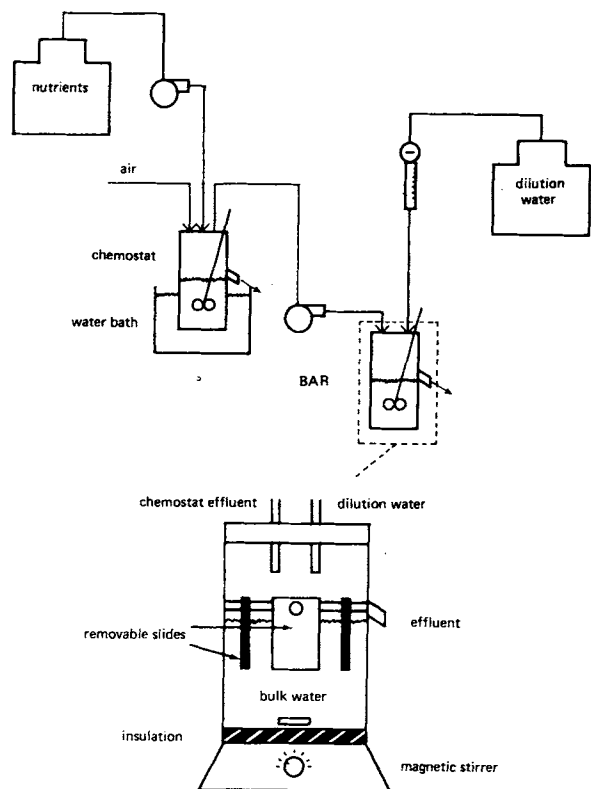


**Figure 1.** Experimental system showing the chemostat where *Pseudomonas* sp. 224S was grown and pumped into the continuous flow bacterial attachment reactor, BAR. Specific growth rate history,  $\mu$ , was varied by adjusting the flow of nutrients through the chemostat. Bulk water concentration,  $X$ , was varied by adjusting the flow of dilution water through the BAR.

culture of *Pseudomonas* sp. 224S was maintained in the chemostat. For the conditions used in this study, 224S had a maximum specific growth rate,  $\mu_m = 0.4 \text{ h}^{-1}$ .<sup>4</sup> The temperature of the chemostat was kept at 20°C. Nutrient and dilution water compositions are listed in Table I.<sup>5</sup> Bacterial growth in the chemostat

**Table I.** Composition of influent nutrients to the chemostat and influent dilution water to the BAR.

Nutrients	
Component	Concentration
$\text{C}_6\text{H}_{12}\text{O}_6$	0.01 g
$\text{NH}_4\text{Cl}$	0.1 g
$\text{Na}_2\text{HPO}_4$	0.56 g
$\text{KH}_2\text{PO}_4$	0.56 g
Trace elements <sup>a</sup>	2.0 mL
Vitamins <sup>a</sup>	0.1 mL
Distilled water	1.0 L
pH	6.8
Dilution water	
$\text{Na}_2\text{HPO}_4$	0.56 g
$\text{KH}_2\text{PO}_4$	0.56 g
Distilled water	1.0 L
pH	6.8

<sup>a</sup> Refer to ref. 5.

was glucose limited. The entire experimental system was autoclaved prior to use.

## METHODS

The variables of interest in this study were the bacterial concentration in the bulk water,  $X$ , and the specific growth rate history,  $\mu$ . Specific growth rate history was varied by adjusting the chemostat dilution rate,  $D$ . Six retention times was presumed sufficient to reach steady state. Bulk water bacterial cell concentration was varied by adjusting the BAR dilution rate,  $F_D$ . 224S was pumped from the chemostat to the BAR at a constant flow rate of 0.3 mL/min for all experiments. The duration of each experiment was 6 h.

The glass microscope slides used in the BAR were cleaned in a consistent manner in order to insure that similar surfaces were used in all experiments. The slides were immersed in tetrachlorethylene for 2 min, transferred to 10% hydrochloric acid for 2 min and rinsed with distilled water. The BAR was washed with 10% HCl and rinsed with distilled water before each experiment.

The slides were exposed to 224S for 6 h and then were removed from the BAR and rinsed with 10 mL of distilled water. The rinse step removed any bacteria which were not "firmly" adsorbed to the surface. The slides were stained with 1 mL acridine orange solution (1 mg acridine orange/mL of 2% formaldehyde) and after a 15-min staining time the slides were rinsed with 10 mL of 70% ethanol and allowed to dry for 10 min. The same glass pipets were used for each experiment in order to minimize potential differences in delivery velocities between pipets. All staining solutions were filtered through 0.22- $\mu\text{m}$  filters.

Adsorbed bacteria were counted using epifluorescence microscopy. Ten fields of  $1 \times 10^{-4} \mu\text{m}^2$  size were counted per slide and reported on a unit area basis. Additional fields were counted if a substantial number of the initial counts were zero. The counts were made in the same relative location on each slide. Both attached bacterial numbers and potential colony forming units (PCFU) were determined. A PCFU is defined as any group of bacteria in physical contact with one another, a bacterium in the process of division, or a single bacterium. The PCFU were counted in order to minimize bias due to cell division in the determination of adsorption rates. The PCFU ranged in size from one to four cells, although over 95% of the PCFU consisted of either one or two cells.<sup>6</sup> An average PCFU value per  $1 \times 10^4 \mu\text{m}^2$  was determined for each experiment by taking an average of counts made from ca. 40 fields from 4 slides.

Chemostat cell counts were determined by epifluorescence microscopy according to the procedure of Hobbie and co-workers.<sup>7</sup> Chemostat cell concentration

remained constant throughout the range of dilution rates used in the study.

## RESULTS

Experiments were designed to facilitate analysis of variance according to Box and co-workers<sup>8</sup> and Hunter.<sup>9</sup> Twelve experiments were arranged in an octagonal design (Fig. 2). The range of each variable was established by preliminary experiments and by limitations

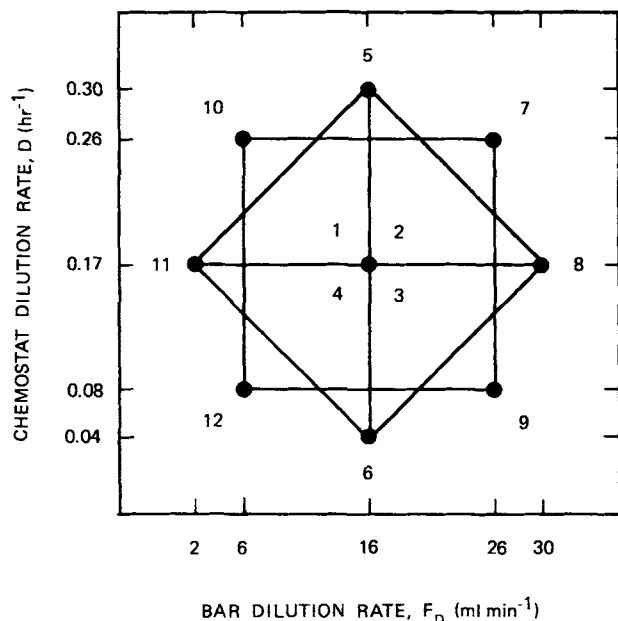


**Figure 2.** Experimental octagon design. Numbered points correspond to individual experiments. Specific growth rate history,  $\mu$ , was varied by adjusting the chemostat dilution rate,  $D$ . Bulk water concentration,  $X$ , was varied by adjusting the BAR dilution rate,  $F_D$ .

of the experimental system. A second order polynomial was proposed as a model to approximate the results. The second order polynomial model is shown in Table II. The resulting analysis of variance table (Table II) indicates the lack of fit of the model to be insignificant at the 5% rejection level and the second-order terms in the model to be significant at the 5% rejection level. In other words, the response surface generated by the proposed second order polynomial model is a statistically valid description of the observed results. Figure 3 compares the response surface generated by the model and the experimentally determined points. The response surface can be described as a "rising ridge."

In order to visualize the response of specific growth rate history,  $\mu$ , on potential colony forming units, PCFU, a cross section of the response surface (Fig. 3) at the midpoint ( $F_D = 16$  mL/min) is presented in Fig. 4. Specific growth rate history,  $\mu$ , in Fig. 4 is equal to the chemostat dilution rate,  $D$ , referred to in Figs. 2 and 3.

## DISCUSSION

Specific growth rate is a measure of the physiological state of a bacterial population. Figure 4 shows the relationship between specific growth rate history,  $\mu$ , and potential colony forming units, PCFU. There appears to be an approximately linear decrease in PCFU as  $\mu$  increases with the maximum number of PCFU occurring at approximately  $\mu = 0.04$  h<sup>-1</sup>. Robinson and co-workers<sup>10</sup> observed in chemostat studies using *Pseudomonas aeruginosa* that the extent of exopolymer accumulation decreased as the specific growth rate of *P. aeruginosa* was increased. This suggests that there may be a direct relationship between the quantity of

**Table II.** Second-order polynomial model and analysis of variance table.

Proposed model:

$$\hat{y} = b_0 + b_1x_1 + b_2x_2 + b_{11}x_1^2 + b_{22}x_2^2 + b_{12}x_1x_2$$

where  $\hat{y}$  is the predicted response;  $x_2$  is the relative value ( $-\sqrt{2}, -1, 0, 1, \sqrt{2}$ ) on vertical scale of octagon design corresponding to the chemostat dilution rate,  $D$ ; and  $x_1$  is the relative value ( $-\sqrt{2}, -1, 0, 1, \sqrt{2}$ ) on horizontal scale of octagon design corresponding to the BAR dilution rate,  $F_D$ .

Analysis of variance table  
(Second-order model,  $K = 2$ )

Sum of squares		DOF	Mean squares	F Ratios
Crude	$S$	56.95	12	
$b_0$	$S_0$	47.60	1	
$b_1, b_2$	$S_{1.0}$	6.24	2	
$b_{11}, b_{22}, b_{12}$	$S_{2.10}$	2.11	3	0.70
Residual = $\Sigma(y - \hat{y})^2$	$S_R$	1.00	6	
Lack of fit	$S_R - S_E$	0.81	3	0.27
Error	$S_E$	0.19	3	0.063
				$F_{3,3} = 11.11$ ( $F_{0.05} = 9.28$ ) (significant)
				$F_{3,3} = 4.29$ ( $F_{0.05} = 9.28$ ) (insignificant)

Second-order polynomial model:

$$\hat{y} = 2.35 + 0.43x_1 - 0.77x_2 - 0.53x_1^2 - 0.004x_2^2 - 0.24x_1x_2.$$

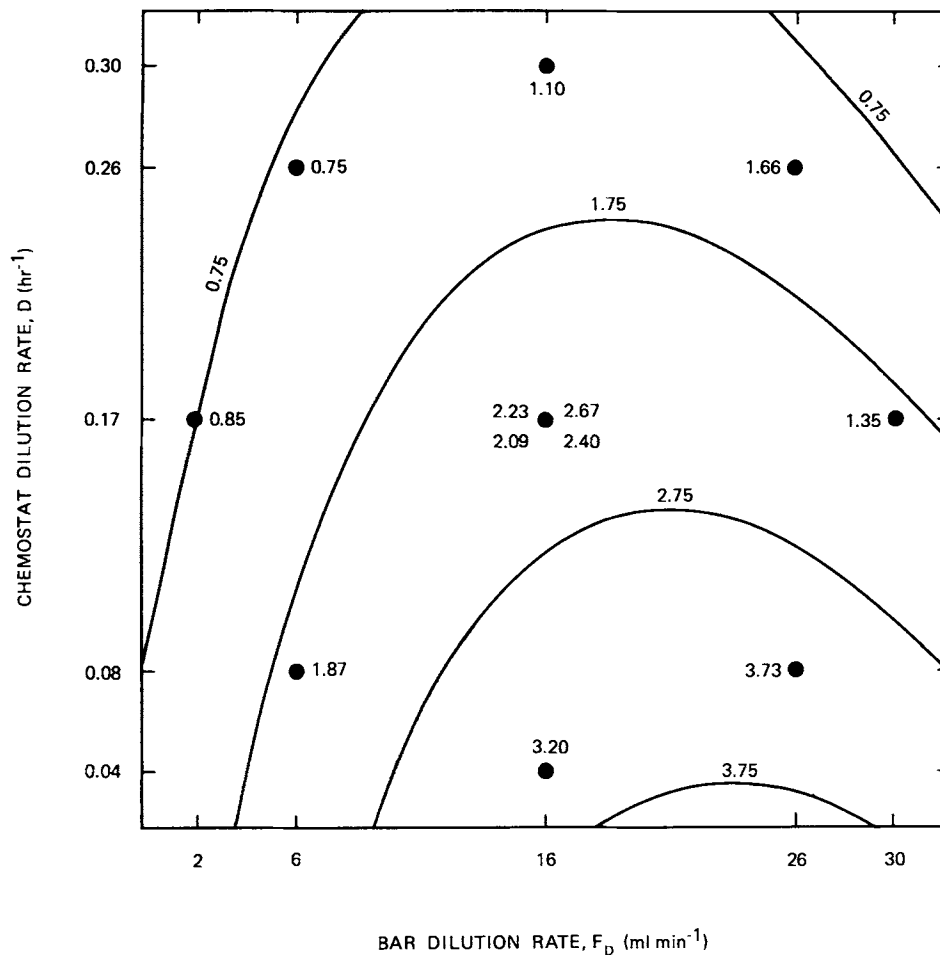


**Figure 3.** Response surface generated by second order polynomial model. Numbers associated with experimental points and response surface lines correspond to PCFU/ $10^4 \mu\text{m}^2$  values. The response surface is a statistically valid approximation of the experimentally determined points.

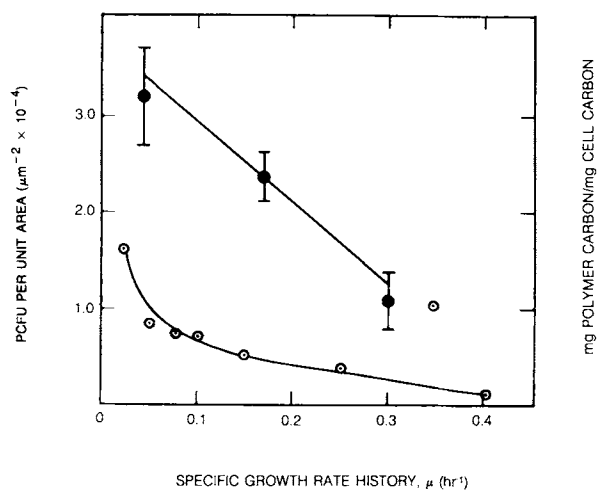


**Figure 4.** Influence of specific growth rate history,  $\mu$ , on potential colony forming units, PCFU. Points (●) and error bars were determined experimentally. The line was generated from a cross section of the response surface in Fig. 3 at  $F_D = 16 \text{ ml min}^{-1}$ . Specific growth rate history,  $\mu$ , is equal to the chemostat dilution rate,  $D$ . Extracellular polymer carbon,  $p$ , per unit cell carbon,  $X$  (○), was reported for *Pseudomonas aeruginosa* by Robinson et al. (1984).

exopolymer produced and adsorption rate, i.e., exopolymers are involved in the adsorption process.

In this study, surface saturation occurred at approximately 0.1% bacterial coverage. Surface saturation has been observed by other investigators. Fletcher<sup>11</sup> observed surface saturation to occur when ca. 40% of the surface was covered with bacteria. Powell and Slater<sup>2</sup> observed surface saturation to occur when ca. 1 or 5% of the surface was covered with bacteria depending on the experimental substratum. The saturation coverage from each study, and calculated transport and accumulation rates, are included in Table III.<sup>2,6,11</sup>

A decrease in sticking efficiency of the bacteria transported to the surface was observed with increasing turbulence. The sticking efficiency can be estimated by calculating the quantity,  $1 - [(\text{rate of transport} - \text{rate of accumulation})/\text{rate of transport}]$ , if attached bacterial growth is insignificant, as was the case in these studies. Decrease in sticking efficiency may be due to differences in the average bacterial residence time at a surface for a given flow regime. For example,

**Table III.** Literature comparisons of saturation coverages and calculated sticking efficiencies.

Flow regime	Percentage coverage at saturation (%)	Rate of transport ( $10^{-4} \times \text{cells/m}^2/\text{s}$ )	Rate of accumulation	Sticking efficiency (%)	Presumed transport mechanism	Reference
Quiescent	40	5000	4170	83	sedimentation	11
Laminar	1	167	31	19	diffusion	2
		472	3	1	diffusion	
Turbulent	0.1	ND <sup>a</sup>	ND	ND	convection	6

<sup>a</sup> ND refers to values that were not determined.

the average bacterial residence time at the surface in Fletcher's quiescent system was on the order of 1 hour and the average bacterial residence time in Powell and Slater's laminar flow system was approximately 5 s.

### SPATIAL DISTRIBUTION

In order to investigate the surface saturation phenomenon further, a spatial pattern test was performed on the experimental data. The spatial pattern test provides a measure of the degree of randomness associated with a population spatial pattern. A spatial pattern is considered random if each unit area of a given surface has the same probability of containing a population member and the occurrence of a population member in any area on the surface does not influence the occurrence of another population member in any area on the surface. There are two possible deviations from the random spatial pattern. The spatial pattern can exhibit clustering, as would occur if individual population members tended to attract each other, or the pattern can exhibit uniformity, as would occur if individual population members tended to repel each other.

The spatial pattern test is based on the Poisson distribution, which describes random occurrences in space or time. If a population is Poisson distributed, the variance,  $\sigma^2$ , of the population counts per area examined equals the mean,  $\mu$ , of the counts,  $\sigma^2/\mu = 1$ , and the population spatial pattern exhibits randomness. If  $\sigma^2/\mu > 1$ , the population spatial pattern exhibits clustering and if  $\sigma^2/\mu < 1$ , the population spatial pattern deviates toward uniformity. Thus, the variance/mean ratio provides an index of the spatial pattern of a population.<sup>12</sup> The sampling distribution of the index allows a statistical test.

The first step in the spatial pattern test is to calculate an index of dispersion, ID:

$$ID = \frac{\sum_{j=1}^n (x_j - \bar{x})^2}{\bar{x}}$$

where

$$\bar{x} = \left( \frac{\sum_{j=1}^n x_j}{n} \right)$$

and  $n$  is the number of microscope fields per experiment and  $x_j$  is the PCFU count in the  $j$ th field. Here, ID is ca.  $\chi^2$  distributed with  $(n - 1)$  degrees of freedom, DOF.<sup>13</sup> The variance/mean ratio,  $\sigma^2/\mu$ , can be approximated by the ratio, ID/DOF. Calculated ID/DOF ratios for each experiment are listed in Table IV.

An ID/DOF ratio for all experiments,  $(ID/DOF)_T$ , was calculated by forming the sum of the ID values from each experiment and dividing by the sum of the DOF values from each experiment to obtain a pooled  $\chi^2$  variate. This was done to increase the number of degrees of freedom, DOF, used in the test. The calculated  $(ID/DOF)_T = 0.90$  from Table IV is obviously less than 1.00, which suggests the PCFU tend toward a uniform spatial pattern. To test whether  $(ID/DOF)_T$  is significantly less than 1.00, the following null hypothesis,  $H_0$ , must be considered;

$$H_0: (ID/DOF)_T \text{ is not significantly less than } 1.00$$

Estimating the probability of  $(ID/DOF)_T = 0.90$  under the null hypothesis required transforming the  $\chi^2$  variate to a standard normal variate,  $z$ , because  $\chi^2$  probability tables for DOF = 696 could not be located:

$$z = (2\chi^2)^{1/2} - (2n' - 1)^{1/2} \quad (3)$$

where

$$\chi^2 = ID$$

**Table IV.** Individual and summed ID, DOF, and ID/DOF values.

Experiment	Index of dispersion (ID)	Degrees of freedom (DOF)	ID/DOF
1	58.51	55	1.06
2	70.93	72	0.99
3	11.33	29	0.39
4	57.17	56	1.02
5	69.20	91	0.76
6	50.33	55	0.92
7	47.58	47	1.01
8	60.08	84	0.72
9	41.62	44	0.95
10	62.16	65	0.96
11	41.32	40	1.03
12	57.18	58	0.99
Totals	627.41	696	0.90

and

$$n' = \text{DOF}$$

For this study,  $z = -1.87$ , which corresponds to  $\alpha = 0.031$  from a normal distribution table. Therefore, the null hypothesis can be rejected at the 3.1% level and the alternative hypothesis of  $(\text{ID}/\text{DOF})_T < 1.00$  can be accepted. A bootstrap experiment confirmed the significance of the test value.

The bacterial surface saturation coverage of ca. 0.1% and the spatial pattern deviation from random in the direction of uniformity might be explained by bacterial oscillations at the surface. Dabrós and van de Ven<sup>14</sup> observed oscillations of negatively charged polystyrene latex particles (0.5  $\mu\text{m}$  diameter) deposited on glass surfaces. The oscillatory motion spanned a few microns during laminar bulk water flow. Dabrós and van de Ven suggested that the particle deposition pattern tended toward uniformity and the oscillating particles could inhibit subsequent deposition of particles from the bulk water in an area 20–30 times the particle cross-sectional area. Dabrós and van de Ven also state that particle oscillations became more pronounced during turbulent bulk water flow. They hypothesize that the mechanism of particle oscillation may involve polymer segments on the order of 10 nm in length protruding from the particle surface and attaching to the test surface. This explanation can be extrapolated to this study since *Pseudomonas* 224S is known to produce extracellular polymers which may be involved in bridging cells to the surface and thus allow oscillations to occur during bulk water flow as suggested by Abbott and co-workers.<sup>15</sup>

## SUMMARY

Adsorption rate of *Pseudomonas* 224S decreases linearly as specific growth rate (history) increases. This trend parallels an observed decrease in extracellular polymer per cell as specific growth rate increased (Robinson and co-workers<sup>10</sup>), which suggests that there is a direct relationship between the quantity of exopolymer per cell and adsorption rates. Surfaces appeared to become saturated to adsorption of bacteria at ca. 0.1% coverage, suggesting that uniform bacterial biofilm development on surfaces is restricted by growth processes rather than transport and attachment processes. The spatial pattern of the adsorbed bacteria

at saturation tended to be uniform rather than clustered or random, suggesting that adsorbed bacteria tend to inhibit subsequent adsorption, in their vicinity, of bacteria from the bulk water.

Financial support from the National Science Foundation (CPE 80-17439), the Office of Naval Research (N00014-80-C-0475), and the Montana State University Engineering Experiment Station is gratefully acknowledged. The authors thank Dr. G. A. McFeters for his constructive comments and M. H. Turakhia for his input on Table III. Dan Goodman is largely responsible for the spatial analysis.

## NOMENCLATURE

$t$	time ( $t$ )
$L$	length ( $L$ )
$X$	bacterial bulk water concentration, cells $L^{-3}$
$\mu$	specific growth rate history ( $t^{-1}$ )
$\mu_m$	maximum specific growth rate ( $t^{-1}$ )
$F_D$	BAR dilution rate ( $L^3/t$ )
$D$	chemostat dilution rate ( $t^{-1}$ )
BAR	continuous flow bacterial attachment reactor
PCFU	potential colony forming units
ID	index of dispersion
DOF	degrees of freedom

## References

1. W. G. Characklis, *Biotechnol. Bioeng.*, **23**, 1923 (1981).
2. M. S. Powell and N. K. H. Slater, *Biotechnol. Bioeng.*, **25**, 891 (1983).
3. P. Rutter and R. Leech, *J. Gen. Microbiol.*, **120**, 301 (1980).
4. J. A. Robinson, personal communication, 1983.
5. P. Gerhardt, R. G. E. Murray, R. N. Costilow, E. W. Nester, W. A. Wood, N. R. Krieg, and G. B. Phillips, *Manual of Methods for General Bacteriology* (American Society for Microbiology, Washington, DC, 1981), p. 98 (21C).
6. C. H. Nelson, "The influence of growth rate and cell concentration on bacterial attachment rates to surfaces in a continuous flow system," M.S. thesis, Montana State University, 1984.
7. J. E. Hobbie, R. J. Daley, and S. Jasper, *Appl. Environ. Microbiol.*, **33**, 1225 (1977).
8. G. E. P. Box, W. G. Hunter, and T. S. Hunter, *Statistics for Experimenters* (Wiley, New York, 1978).
9. J. S. Hunter, *Chem. Eng. Prog. Symp. Ser. No. 31*, **56**: 1 (1960).
10. J. A. Robinson, M. G. Trulear, and W. G. Characklis, *Biotechnol. Bioeng.*, **26**, 1409 (1984).
11. M. Fletcher, *Can. J. Microbiol.*, **23**, 1 (1977).
12. J. H. Zar, *Biostatistical analysis* (Prentice-Hall, Englewood Cliffs, NJ, 1974), pp. 301–305.
13. E. C. Pielou, *Mathematical Ecology* (Wiley, New York, 1977), pp. 124–126.
14. T. Dabrós and T. G. M. van de Ven, *Colloid Polym. Sci.*, **261**, 694 (1983).
15. A. Abbott, P. R. Rutter, and R. C. W. Berkeley, *J. Gen. Microbiol.*, **129**, 439 (1983).